Journal of Structural Geology, Vol. 11, No. 6, pp. 657 to 667, 1989
Printed in Great Britain

0191-8141/89 $03.00+0.00

Experimentally produced slickenside lineations in pyrophyllitic clay

T. M. WILL and C. J. L. WILSON

Department of Geology, The University of Melbourne, Parkville, Victoria 3052, Australia

(*Received* 7 *October* 1988; *accepted in revised form* 16 *March* 1989)

Abstract—During shearing of pyrophyllitic clay, fault planes bearing slickenlines were generated on previously initiated *C*- and *C'*-planes. These slickenlines have excess lengths with respect to the measured slip displacement on the fault plane and are of the ridge-in-groove type with the hangingwall nesting into the footwall, and vice versa. These features cannot be explained in terms of either frictional asperity ploughing or dissolution/reprecipitation but are produced during the development of a complex ductile shear zone that contains the fault plane. This initial shear zone nucleates from localized shear bands that link up to form a throughgoing shear plane. The nucleation and propagation of the fault post-dates the formation of the shear plane and depends on the development of a zone of highly oriented layer silicates within the pyrophyllitic clay. The fault is confined to this zone. The lineations observed on the fault surfaces are produced while the material behaves plastically prior to the brittle faulting. With increasing shear strain the brittle–ductile transition is crossed and sliding continues under brittle conditions along the former shear zone.

INTRODUCTION

SLICKENSIDES have been defined as "polished and smoothly striated surfaces that result from friction along the fault plane" (Gary *et al.* 1977, p. 665). The concept that brittle deformation, friction and asperity ploughing (Engelder 1974) are the sole processes involved in the formation of slickensides on planar surfaces is contradicted by recent observations that slickenside lineations, slickenlines in the terminology of Fleuty (1975), can be related to *C*-planes within ductile shear zones as in deformed granitoid plutons (Burg & Ponce de Leon 1985, Burg & Wilson 1988). If these slickenlines developed contemporaneously with the shear zone then this suggests that slickensides and accompanying slickenlines can form under more ductile conditions than generally believed. During this study it became clear that mechanisms other than frictional polishing can be involved in the formation of slickensides and these processes will be described here.

The slickenside lineation of the "ridge-in-groove" type (Means 1987) is a likely candidate for having nucleated under non-brittle conditions, and is described in this study. The ridge-in-groove type lineation is characterized by: (i) slip-parallel planar segments that link up to form shallow ridges and grooves on a fault surface (Means 1987); (ii) nesting of ridges and grooves with a footwall groove fitting into a hangingwall ridge, and vice versa (Means 1987); and (iii) that the length of individual ridges and grooves can exceed the amount of the slip displacement (Will 1987).

EXPERIMENTAL PROCEDURE

The experiments were carried out using a pyrophyllitic clay (of grain size 10–50 μm) composed of a pyrophyllitic powder and water in the ratio 4:1 by weight. The powder was produced by grinding solid pyrophyllite rock, purchased from the American Lava Company under the trade name "Lava Grade A", with glasspaper. The compacted mixture was placed in the sample holes (20 × 10 × 12.7 mm) of the double-shear jig described by Means (1987, fig. 1). Horizontal marker lines or grids were scratched on the front and back faces of the pyrophyllitic clay samples and filled with white talcum powder. After the samples had been loaded into the jig either steel or glass plates were clamped on the front and rear of the deformation apparatus to prevent leakage. The jig was mounted on the fixed lower platen of a motor driven Carver Laboratory Press, Model C. The upper platen pushed down the plunger of the double-shear jig to achieve shear strain rates on the sample scale of 10^{-3}–10^{-5} s^{-1}. The direction of displacement was parallel to the long edge of the sample. Experiments were performed at room temperature and did not exceed 3 h; in most experiments the material was deformed for 20–45 min. Due to the compaction of the clay void spaces opened up at the jig–sample interface during deformation.

The marker lines were used to determine: (i) the magnitude of the total displacement, d_t, that is the separation distance between marker lines at the outer edges of the sample; (ii) the slip displacement, d_s, which is the amount of offset along the slip surface; and (iii) the shear strain, γ, averaged across the specimen (Fig. 1). In the center of some samples a surface was cut normal to the slip direction and a talcum marker plane was incorporated into the sample.

To establish whether the experimentally-produced slickenlines are of the ridge-in-groove type lineation the following reversed print technique was applied. After an experiment the faulted samples (Fig. 2a) were photographed using the same light source and illumination angle (Figs. 2b & c); the footwall surface from the left, and the hangingwall surface from the right side. Surface

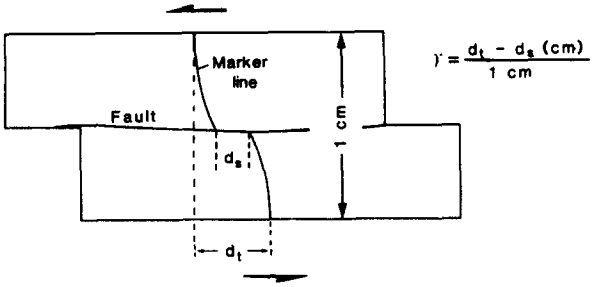

Fig. 1. Measurement of total displacement, d_t, slip displacement, d_s, and shear strain, γ, using a marker line on a deformed sample.

segments with normals that bisect the angle between the light and the camera lens are brightly illuminated on the photograph. Surface segments inclined away from this position reflect less light, and hence became darker on the final photograph (Figs. 2d & e). The photograph of one fault surface was reversed by placing an undeveloped sheet of photographic paper under the developed print and the two emulsion sides in contact upon development of the reversed print. The dark area on the original print becomes bright on the reversed print, and vice versa (Figs. 2f & g). If hangingwall and footwall surfaces nest across a fault plane then the reversed print of the footwall and the original print of the hangingwall, or vice versa, should be identical.

Photographs were also used to measure the horizontal distance between two planar segments of ridges or grooves that reflected light with the same intensity (e.g. the distance A–B in Fig. 2d). This is the reflection distance, R_d. Across the fault, surface profiles were taken perpendicular to the slip direction, and the number of either the bright or the dark strips was counted. The total number measured was divided by the profile length, and a mean reflection distance, R_d, was calculated.

Samples were impregnated with 'Spurr low-viscosity' embedding media, sectioned and thinned to some 25 μm thickness for optical microscope observations. Scanning electron microscope (SEM) observations of fault surfaces were undertaken on an ISI Mini-SEM.

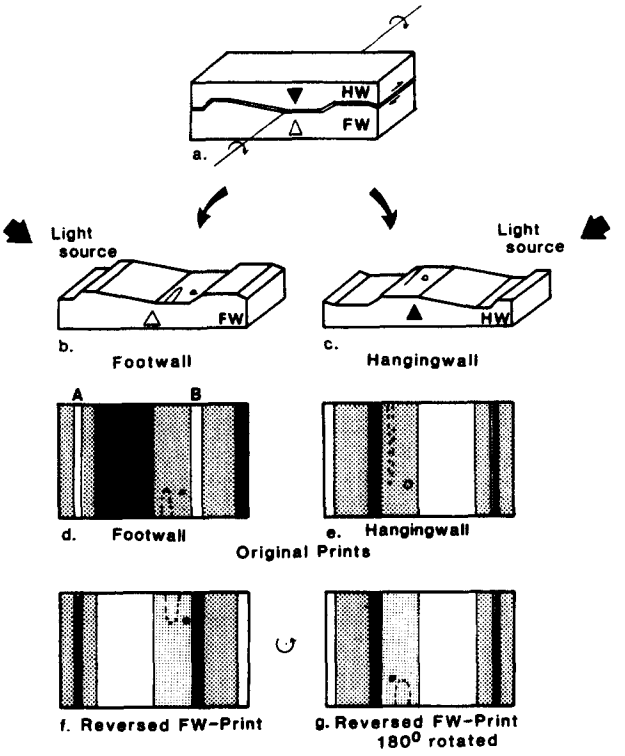

Fig. 2. Reversed print technique for assessing the degree of nesting between ridges and grooves from hangingwall (HW) and footwall (FW) surfaces. The direction of displacement is indicated by the arrows (a). The two blocks in (a) are opened up by rotating about an axis parallel to the slip direction and are illuminated as indicated by the short arrows (b & c). Distribution of dark and bright stripes represents the different orientations of the individual fault plane segments (d & e). Reversed print of the footwall (f), and rotated by 180° (g). If two surfaces nest, then the reversed print will be identical to the original print of the hangingwall (e & g). Striations of an abrasional origin (dashed lines) are not identical on the reversed footwall and original hangingwall surfaces, and do not nest.

RESULTS

Strain distribution

At small magnitudes of displacement the paired samples in the double jig, deformed under identical conditions, display similar surface and internal features. There is a heterogeneity in strain distribution parallel to the long edge of the sample. Marker grids indicated different responses of the pyrophyllitic material to increasing shear strain at different positions parallel to the long edge of the sample. Comparison of marker line positions at the edge of the sample indicate an offset while in the center of the sample marker lines are bent in a sigmoidal fashion, until they become offset after the nucleation of the fault plane. As indicated by the open voids at the end of the samples (Fig. 3) compaction must have occurred in the material adjacent to the voids.

Comparison of samples at higher displacement (>2 mm) can reveal local differences in individual sample response to deformation such as the number, length and location of shear bands that develop in the centrally sheared section of the sample. As a consequence of the local inhomogeneities of strain, a fault may start to propagate in one sample at a particular instant but not at the same time in the other sample.

Features of the slickensides

Nesting lineations of the ridge-in-groove type (Means 1987, Will 1987) were produced during the experiments. For example, a print of the footwall surface (Fig. 4a) was reversed (Fig. 4c) to reproduce optical features that are comparable in length and width to those observed on the corresponding hangingwall surface (Fig. 4b). Along a common profile line on the fault surface, small-scale ridges (lighter lines) and grooves (darker lines) (Fig. 4d) can be correlated from the footwall to the hangingwall.

Comparison of the slip displacement, d_s, on a fault surface, as measured from the offset marker line (verti-

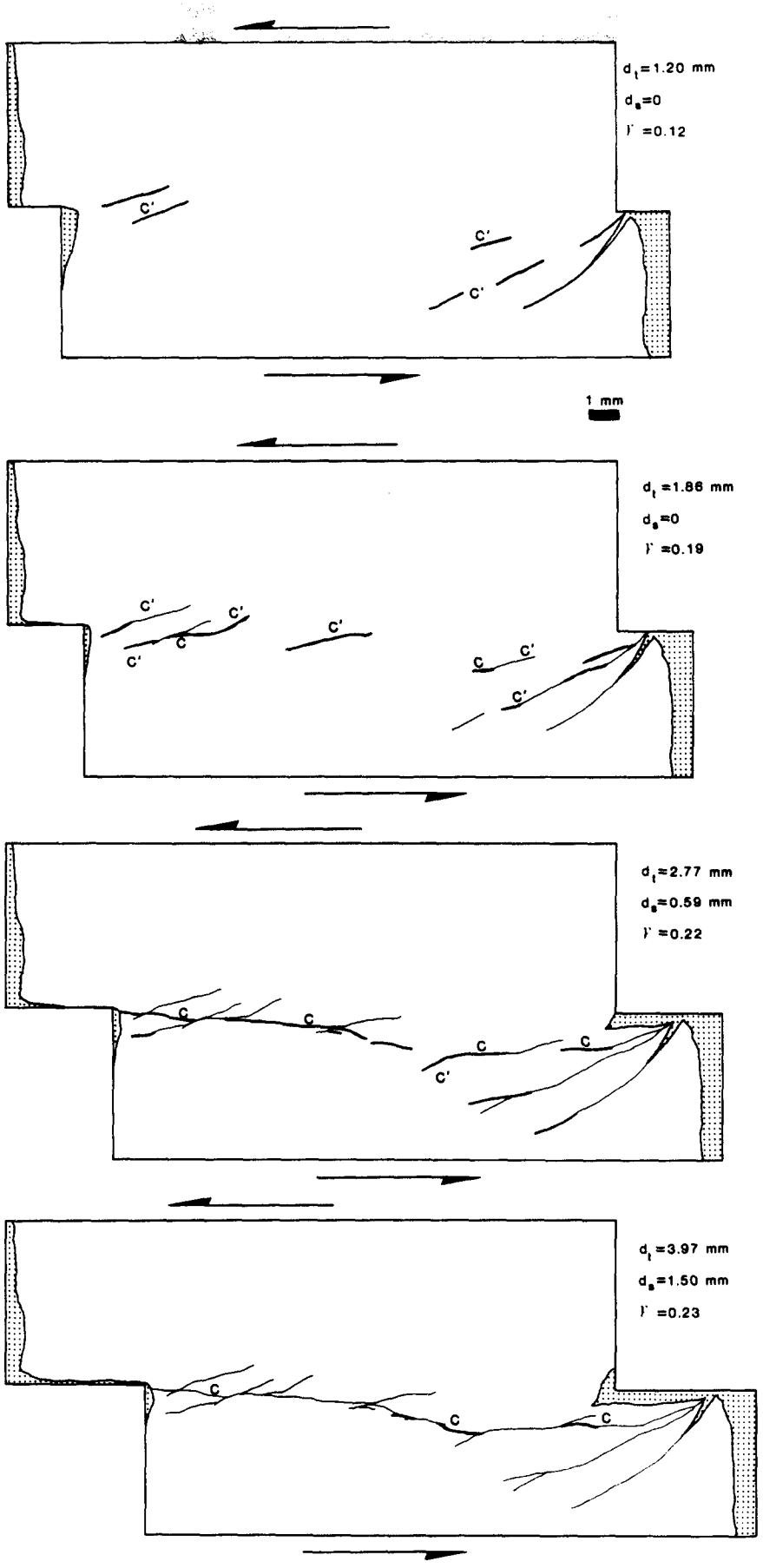

Fig. 3. (a–d) Development of a throughgoing fault plane on *C*- and *C'*-planes, sketched from photographs of experiment PS-065-R. The stippled areas are voids developed during shearing. Heavy lines denote new fault plane segments developed at the instant shown; light lines indicate fault plane segments already present at this time.

cal bar in Fig. 5a), and the maximum length of the grooves (between the black arrows in Fig. 5a) shows that the grooves can have an excess length. Similar observations have been made by Hobbs *et al.* (1976, p. 303). The grooves are continuous and parallel to the direction of the slip vector. All marker planes intersect the fault as straight lines and show no curvature at any scale, which indicates a homogeneous strain distribution across the entire width of the sample. Identical ridge and groove lengths for the same slip displacement, d_s, were recorded from both samples taken from the double jig.

The excess length is most prominent immediately after a fault has formed and decreases approximately exponentially with increasing slip displacement (Fig. 6). Measurements were only recorded from the center of the sample, as ridges and grooves that were nucleated at the edges, adjacent to the advancing plunger, were destroyed with progressive deformation. At higher shear strains more than one surface may truncate the throughgoing fault surface (Fig. 5b) and it becomes difficult to measure the length of the individual ridges and grooves because they disappear under other surfaces.

Mean reflection distances recorded do not change significantly with slip displacements greater than 1 mm (Fig. 7a). This suggests that ridge and groove widths are nearly constant with increasing strain. No data could be obtained for slip displacements of less than 1 mm because no throughgoing fault plane was present and the samples could not be parted. At constant slip displacement the mean reflection distance is insensitive to varying shear strain rate (Fig. 7b).

Sections across the fault surface

During deformation the initial orientation of the pyrophyllite particles (Fig. 8a) is changed and the layer silicates become aligned in a strain-modified zone, up to 4 mm wide, along the median plane of the sample. This zone is defined by oriented grains of pyrophyllite as narrow shear zones and shear bands (up to 60 μm wide). The geometrical orientation of the zone of aligned pyrophyllite with respect to the fault surface corresponds to that of *R*-shears (Riedel 1929), an extensional crenulation cleavage (Platt 1979) or shear bands, *C'*. Because of the obvious ductile behavior of the pyrophyllitic clay during the first increments of deformaton, as indicated by the sigmoidal bending of the marker lines, these slip surfaces are described as shear bands, *C'*, rather than as *R*-shears. For the same reason the main fault plane is described as a *C*-plane.

The first nucleation of the shear bands was always near the edges of the sample and prior to the development of the *C*-planes (Fig. 3a). Further displacement (Figs. 3b & c) produces more shear bands that link up to form the main fault surface (Fig. 3d). The main fault surface is dominated by large planar areas upon which lie the excess-length slickenlines. In a plane containing the slip vector and perpendicular to the fault plane (Fig. 9) these planar surfaces are cut by *C'*-shear bands to produce a step-like appearance that corresponds to a normal fault displacement on the shear bands.

The microstructural characteristics can be seen best in sections parallel to the slip vector (Fig. 8b) where the (0001) traces of the pyrophyllite particles are dipping at a shallower angle and slightly oblique to the shear band boundaries. The shear bands are inclined at a shallow angle of some 15–20° to the main shear plane and are identified by the strong preferred orientation of layer silicates.

Perpendicular to the slip direction, the strain-modified zone can be recognized by the alignment of layer silicates in bands across the sample in an otherwise randomly oriented matrix. Individual bands are interpreted to be *C'*-planes being part of a larger *C'*-zone in which the *C*-plane develops. The orientation of the (0001) traces in the shear bands varies between 0 and 40° with respect to the shear band boundaries. The *C*-plane

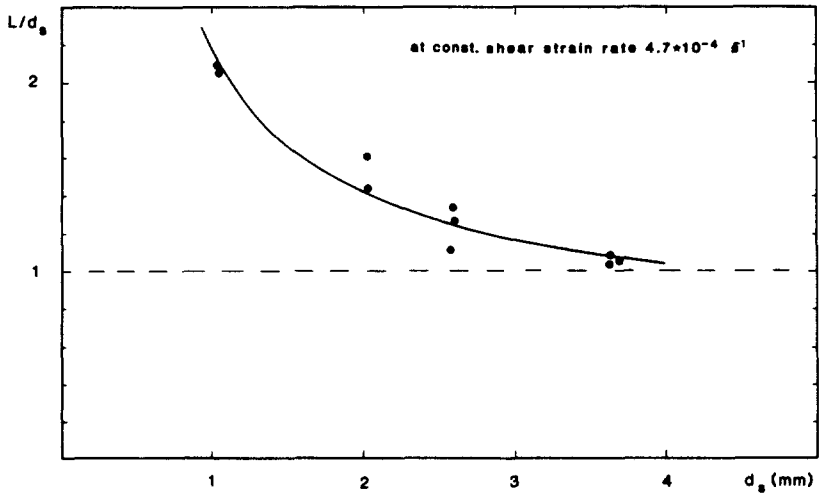

Fig. 6. Maximum ridge-and-groove length/slip-displacement ratio vs slip displacement for a constant shear strain rate of 4.7×10^{-4} s^{-1}. Length measurements were recorded from the central areas of the fault surfaces. L is the length of the lineation, d_s the slip displacement.

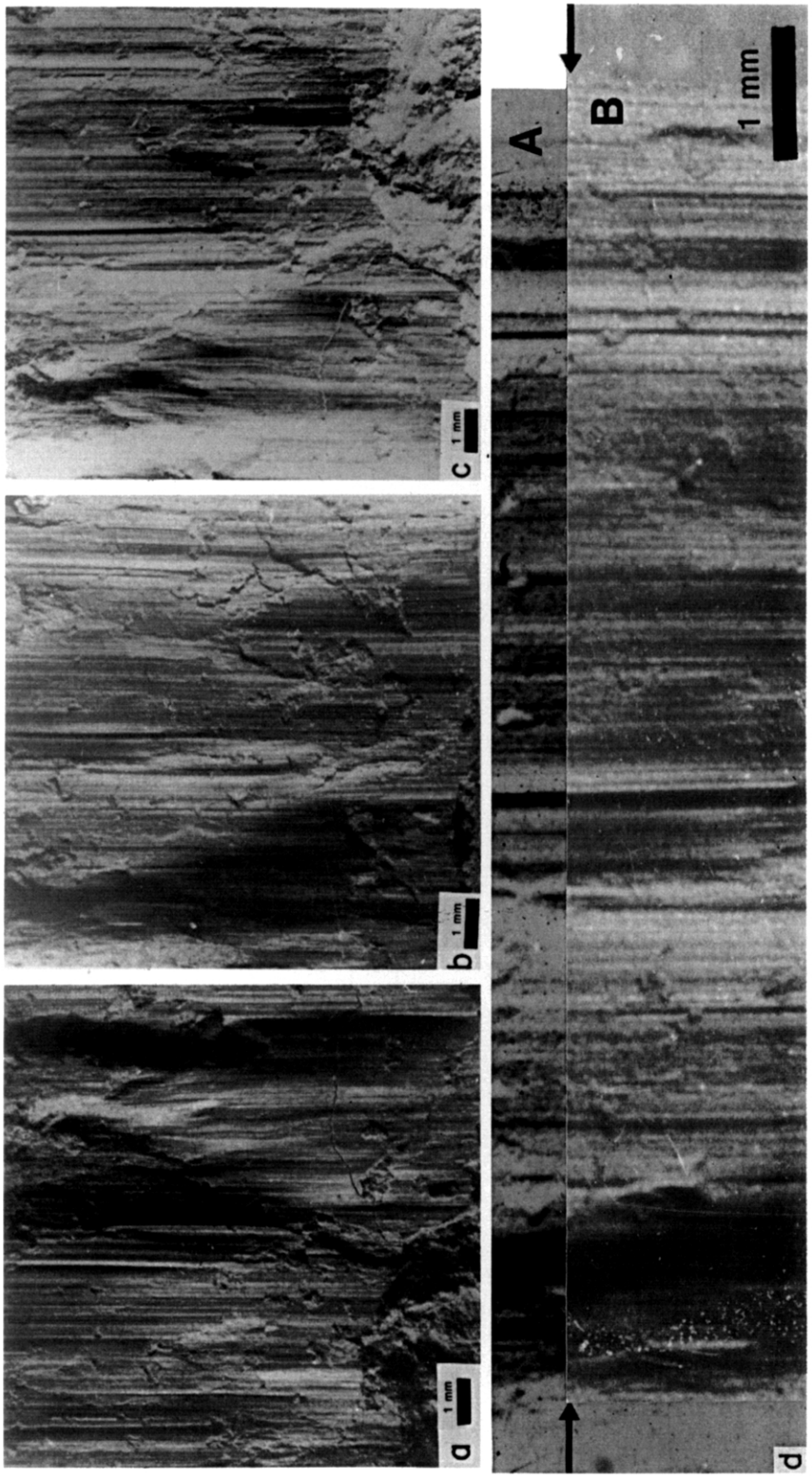

Fig. 4. Surface features associated with sample PS-051-LL, after a slip displacement of 5.0 mm. (a) Footwall. (b) Hangingwall. Nesting is demonstrated by the close match of the reversed print of the footwall (c) and the original print of the hangingwall (b). (d) Corresponding areas adjacent to a common profile line (arrows) on the sliding surface shown in (b & c). A is the reversed print of the footwall and B is the original print of the hangingwall. Note that almost all of the lineations can be traced from one photograph to the other, and hence show nesting. The hangingwall moved down with respect to the footwall. $\gamma = 0.37$.

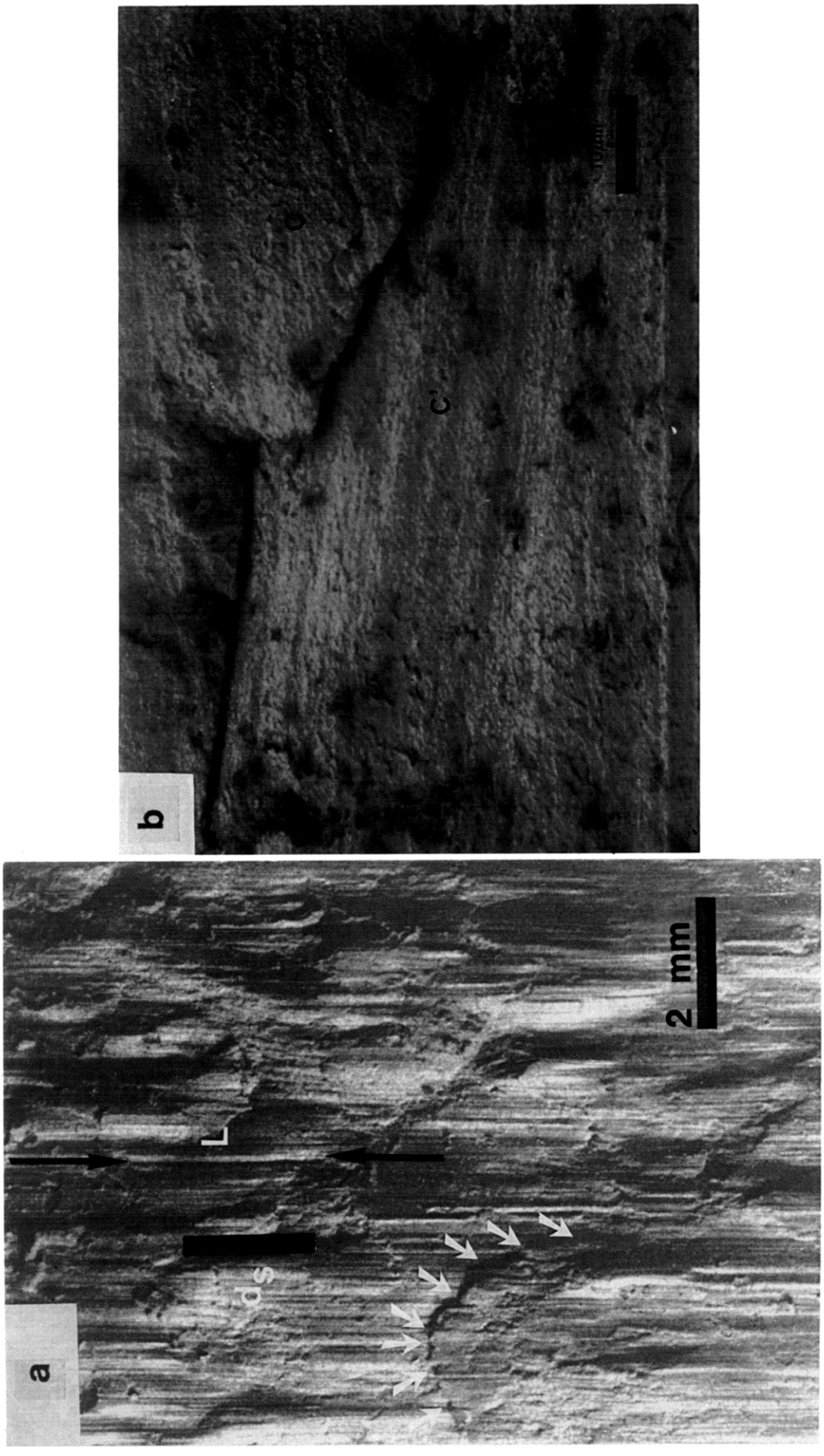

Fig. 5. (a) Demonstration of excess length (between black arrows). The upper, removed block moved down with respect to the sample shown. The white arrows point to a trace of a *C'*-plane on the fault plane. The *C'*-plane truncates the *C*-plane. Experiment PS-057-RL, slip displacement 2.0 mm. $\gamma = 0.25$. (b) Striated fault planes in *C*- and *C'*-plane orientations. Sample PS-051-LR. SEM photomicrograph. The removed hangingwall block moved to the right. $\gamma = 0.37$

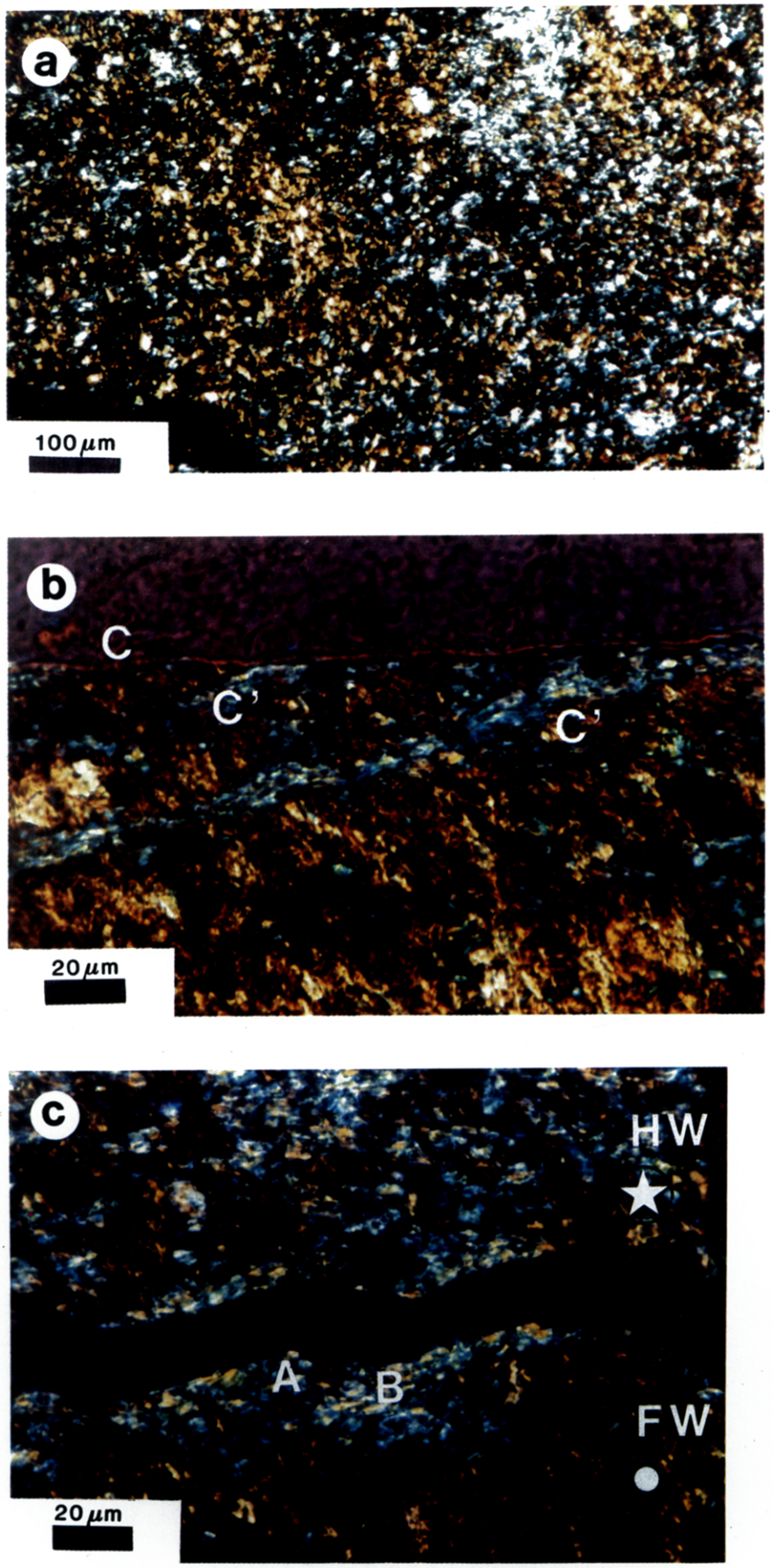

Fig. 8. (a) Undeformed reference sample of pyrophyllitic clay. After inserting the gypsum plate domains of dominantly yellow and blue colors can be recognized in an otherwise randomly colored matrix. This indicates that no truly random fabric could be achieved during sample prepartion (which is almost impossible to establish due to the platy shape of the grains and the compactional strains involved during sample preparation). More importantly, however, no overall preferred alignment of layer silicates is visible in the undeformed sample. Crossed polarizers, gypsum plate. (b) Shear-induced strain-modified fabric in a view parallel to slip direction. Experiment PS-056-RL. The material at the top of the photomicrograph is epoxy. Crossed polarizers, gypsum plate, $\gamma = 0.25$. (c) View perpendicular to the slip direction (sample PS-068-LL). Minor ridges (at A) and grooves (at B) are present. The footwall (FW) moved towards the viewer. The material in the center of the photograph infilling the slip surface is epoxy. Crossed polarizers, gypsum plate, $\gamma = 0.53$.

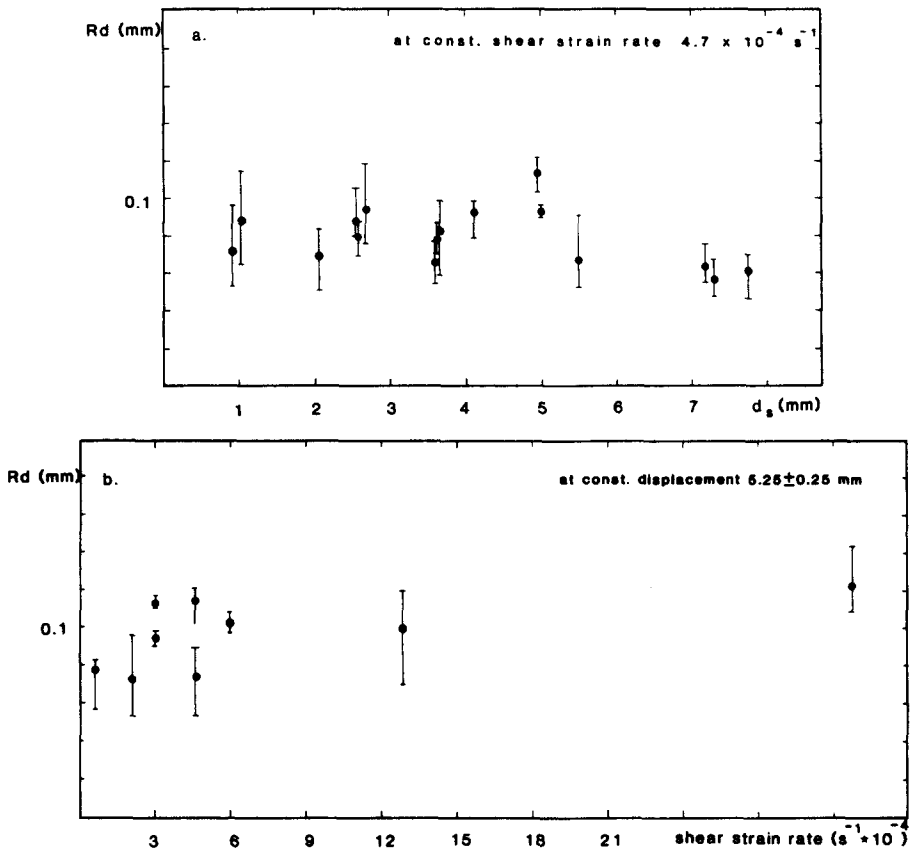

Fig. 7. Mean reflection spacing, R_d, as a function of slip displacement at a constant shear strain rate of $4.7 \times 10^{-4} s^{-1}$ (a) and shear strain rate at a constant slip displacement of 5.25 ± 0.25 mm (b). The solid dots correspond to the mean spacing, and the bars indicate the observed range of spacings.

is composed of minor ridges (at A in Fig. 8c) and grooves (at B in Fig. 8c). These minor undulations (sometimes smaller than 10–20 μm) very likely correspond to layer silicates oriented obliquely to the shearing surface at A and sub-parallel at B (Fig. 8c). These small-scale ridges and grooves appear to be the very fine lineations observed on both C- and C'-planes (Fig. 5b). The presence of the lineations suggests that both surfaces were shear planes and that pyrophyllite particles were being realigned parallel to this direction.

DISCUSSION

The faulted surfaces produced in the pyrophyllitic clay are nesting surfaces of the ridge-in-groove type bearing excess length lineation whose formation cannot be explained by the asperity ploughing model.

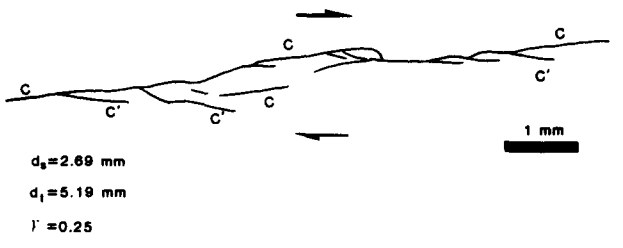

Fig. 9. Sketch of the fault surface, C, and shear bands, C', as observed in sample PS-056-RL. $\gamma = 0.25$.

Heterogeneous displacement on the fault plane, to explain the development of the excess length feature, is not supported by the observed displacement of marker planes. This excess length feature is in contrast with Engelder's (1974) carrot-shaped wear grooves that were equal in length or shorter than the recorded slip displacement.

There is no significant change in reflection distance between ridges and grooves with shear strain rate (Fig. 7a) and/or slip displacement (Fig. 7b). The absence of data at low slip displacements and low shear strain rates might indicate that at least two different processes may be involved in the formation of the lineations. At low slip displacements and/or low shear strain rates ductile shearing occurs along the C'-planes and the developing C-plane segments and the lineations start to form. At a certain instant the throughgoing C-plane has been established and further sliding is confined to this plane. This is in agreement with the observations that at least two different deformational stages are present in sequence (i.e. before and after the final development of the throughgoing shear plane).

A sequential development is proposed for the formation of the ridge-in-groove type lineation (Fig. 10) based on the following experimental observations: (i) lineations developed on planes in C- and C'-plane orientations; (ii) open voids formed at the ends of the samples; (iii) C'-planes developed first at the sample ends and prior to the C-planes; (iv) the marker lines at

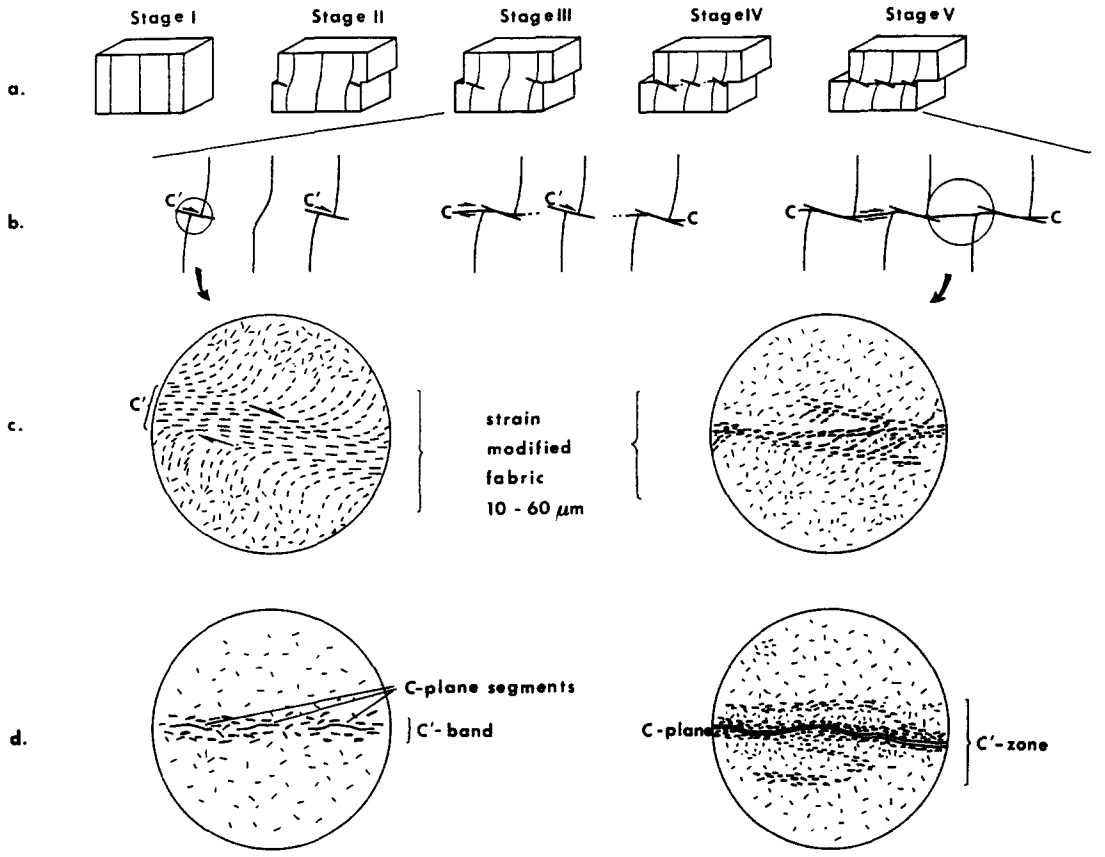

Fig. 10. Summary of the main microstructural features as observed during the shearing of pyrophyllitic clay. (a) Temporal sequence for the development of the fault plane and associated ridge-in-groove type lineation in an experimentally deformed sample. (b) Enlargement of the stages III–V in (a). The arrows indicate the accommodation of strain on particular slip planes during deformation. (c) View parallel to the sliding direction and perpendicular to the slickenside. At stage III active shear bands, *C'*, are developed, whereas at stage V the shear bands are inactive and deformation on the *C*-plane is dominant. (d) View perpendicular to the lineation and perpendicular to the slickenside. At stage III a shear band with nucleated and propagating *C*-plane segments is present. At stage V a *C'*-zone has developed enclosing the fully developed, active *C*-plane.

the outside of the samples became sigmoidally bent prior to their offset; (v) excess length lineations occur; and (vi) a strain-modified fabric was recognized in thin section.

Deformation in the shear bands localized towards the ends of the samples cannot accommodate progressively increasing shear strain, and the *C*-plane, which will become the main fault surface, is initialized (Figs. 3 and 10a & b). It is suggested that the initiation of the final slip on a *C*-plane will occur preferentially at positions where the (0001) planes of the layer silicates are more or less aligned parallel to the bulk slip direction. This implies that the nucleation and propagation of the *C*-plane segments will start in localized zones of high shear strain concentrations throughout the sample.

In a view perpendicular to the slip vector (Fig. 10d), already nucleated *C*-plane segments are shown within a *C'*-zone. It is suggested that when *C*-plane segments propagating along slip-parallel (0001) planes come to layer silicates whose (0001) planes are inclined to the orientation of the propagating *C*-plane segment, this *C*-plane segment will propagate along the (0001) planes of those inclined segments which offer the least resistance to sliding, and thus will change orientation. This will preferentially happen where the (0001) planes of the pyrophyllite flakes are subparallel to the slip plane and parallel to the slip vector. *C*-plane segments will propagate along these layer silicates within the *C'*-zone until either two propagating segments link up and form a lateral ramp or the propagating *C*-plane segment meets an oriented group of layer silicates that facilitate further sliding at a slightly oblique angle with respect to the previous sliding direction.

An explanation for the propagation of ridges and grooves parallel to the slip vector might be that layer silicates become progressively rotated and oriented into a plane approximately coincident with the layer silicate orientation within the *C'*-bands. This facilitates further slip-parallel propagation of the ridge-in-groove shaped *C*-plane. Clusters of grains, highly misoriented to the slip-parallel propagation direction might lead to an abrupt ridge or groove termination, or to the occasionally observed feature that ridges turn into grooves, and vice versa.

If the material is no longer able to accommodate the increasing shear strain by continued ductile deformation the brittle–ductile transition is crossed into a brittle sliding regime where sliding will take place along the

former C-plane and will continue until it becomes geometrically locked. In this case additional C'-surfaces are nucleated and the process is repeated to produce multiple C- and C'-slip surfaces subparallel to the main sliding surface.

CONCLUSION

Movements on fault planes are indicated by slickenside lineations consisting of ridges and grooves parallel to the direction of movement and it is commonly thought that these originate solely by brittle processes (Gary *et al.* 1977, p. 665). However this investigation demonstrates that the ridge and groove formation associated with slickensides in layer silicate rich rocks can occur while the material behaves plastically and is not related to a frictional sliding process. It is localized ductile shearing that produces the ridge-in-groove type lineation. These begin to develop prior to any transition into a brittle sliding regime and the physical offset of the marker lines. The excess length and the nesting between footwall and hangingwall ridges and grooves is therefore a product of this plastic deformation. The idea that a measured length of either a ridge or groove could be an indicator of the magnitude of slip displacement is questionable as lengths are a function of the rheological parameters of any material sheared involving grain rotation and localization of strain to particular C'-bands. The partitioning of strain, experienced by the sample, into different C'-bands produces a cumulative localization of strain that eventually leads to the formation of the C-planes upon which faulting may occur.

The initiation of a fracture, faulting and a transition into brittle deformation conditions will occur after the cohesive bonds between layer silicates across the future fault plane have been broken. As less shear stress is necessary for slip to continue along an already present discontinuity than along the still intact material, further frictional sliding will occur along the former C-plane and the ridge-in-groove shape morphology will be preserved.

From the observations made, the following slickenside definition is proposed: a slickenside is a "strain-modified zone of variable thickness at a slip plane, whose surface displays any kind of markings produced during displacement on this surface". This definition has the advantage that it includes slickensides produced at the brittle–ductile transition and, furthermore defines a slickenside without any genetic connotations, as implied by the traditionally used terms "frictional" or "polished". A slickenside of the type described above might be called a "slickenside *sensu lato*" whereas a slickenside fitting the traditional definition, "polished and smoothly striated surface that results from friction along a fault plane" (Gary *et al.* 1977, p. 665) might be called a "slickenside *sensu stricto*".

Acknowledgements—This work was supported by the National Science Foundation grant EAR 860961 to W. D. Means. W. D. Means is thanked for numerous discussions on the subject while C. J. L. Wilson was on study leave and one of us (T. M. Will) completed his M.Sc. project on slickenside development under his supervision at SUNY Albany. This work was undertaken while one of us (T. M. Will) held a fellowship of the 'Studienstiftung des Deutschen Volkes'.

REFERENCES

Burg, J. P. & Ponce de Leon, M. I. 1985. Pressure-solution structures in a granite. *J. Struct. Geol.* **7**, 431–436.

Burg, J. P. & Wilson, C. J. L. 1988. A kinematic analysis of the southernmost part of the Bega Batholith. *Austr. J. Earth Sci.* **35**, 1–13.

Engelder, J. T. 1974. Microscopic wear-grooves on slickensides: indicators of paleoseismicity. *J. geophys. Res.* **79**, 4387–4392.

Fleuty, M. J. 1975. Slickensides and slickenlines. *Geol. Mag.* **112**, 319–322.

Gary, M., McAfee, R. Jr. & Wolf, C. L. (eds) 1977. *Glossary of Geology*. American Geological Institute, Washington, D.C.

Hobbs, B. E., Means, W. D. & Williams, P. F. 1976. *An Outline of Structural Geology*. Wiley, New York.

Means, W. D. 1987. A newly recognized type of slickenside striation. *J. Struct. Geol.* **9**, 585–590.

Platt, J. P. 1979. Extensional crenulation cleavage. *J. Struct. Geol.* **1**, 95–96.

Riedel, W. 1929. Zur Mechanik geologischer Bruchcrscheinungen. *Zentbl. Miner. Geol. Paläont.* **1929B**, 354–368.

Will, T. M. 1987. Structural investigations on experimentally and naturally produced slickensides. Unpublished M.Sc. thesis, State University of New York at Albany.